SLAC–PUB–7392
Jan 1997

Initial Commissioning Results of Next Generation Photoinjector*

D. T. Palmer*, X. J. Wang†, R. H. Miller*
M. Babzien†,I. Ben-Zvi†, C. Pellegrini**, J. Sheehan†,
J. Skaritka†, H. Winick*, M. Woodle†, V. Yakimenko†

*Stanford Linear Accelerator Center
Stanford University, Stanford, CA 94309

†Brookhaven National Laboratory
Accelerator Test Facility
Upton, NY 11973

**University of California Los Angeles
Department of Physics
Los Angeles, CA 90095

Abstract

The Next Generation Photoinjector(NGP) developed by the BNL/SLAC/UCLA collaboration has been installed at the Brookhaven Accelerator Test Facility(ATF). The initial commissioning results and performance of the photocathode injector are presented. The NGP consists of the symmetrized BNL/SLAC/UCLA 1.6 cell S-band photocathode RF gun and a single solenoidal magnet for transverse emittance compensation.[1] The highest acceleration field achieved on the cathode is 150 $\frac{MV}{m}$, and the normal operating field is 130 $\frac{MV}{m}$. The quantum efficiency of the copper cathode was measured to be 4.5x10^{-5}. The transverse emittance and bunch length of the photoelectron beam were measured. The optimized rms normalized emittance for a charge of 300 pC is 0.7 π mm-mrad. The bunch length dependency of photoelectron beam on the RF gun phase and acceleration fields were experimentally investigated.

Contributed to
7th Advanced Accelerator Concepts Workshop
Lake Tahoe, CA, USA
Oct 12–Oct 18, 1996

*Work supported by Department of Energy contract DE–AC03–76SF00515.

1 Introduction

The Next Generation Photoinjector(NGP) has been installed at the Brookhaven Accelerator Test Facility(ATF) as the electron source for beam dynamics studies, laser acceleration and free electron laser experiments. The injector consists of the symmetrized BNL/SLAC/UCLA 1.6 cell S-band photocathode RF gun, powered by an XK-5 klystron, and is equipped with a single emittance compensation solenoidal magnet. There is a short drift space between the NGP and the input to the first of two SLAC three meter travelling wave accelerating sections. This low energy drift space contains a copper mirror that can be used in either transition radiation studies or laser alignment. There is also a beam profile monitor/faraday plate located 66.4 cm from the cathode plane.

The ATF consists of two SLAC travelling wave linacs powered by a single XK-5 klystron. The high energy beam transport system consists of nine quadrupole magnets, an energy spectrometer, an energy selection slit and a high-energy faraday cup. Diagnostics located in the high energy transport consist of beam profile monitors and strip lines. The strip lines are used for an on line laser/RF phase stability monitor.

The drive laser is a Nd:YAG master oscillator/power amplifier system. A diode pumper oscillator mode locked at 81.6 MHz producing 21 psec FWHM pulses at 100 mW of average power. Gated pulses seed two flashlamp pumped multi-pass amplifiers and are subsequently frequency quadrupled. This nonlinear process leads to a factor of two reduction in the laser pulse length. The 266 nm beam is transported to the RF gun area via a 20 meter long evacuated pipe. The laser beam transport system near the injector includes an aperture, a set of telescoping lenses and a limiting aperture. This limiting aperture is imaged onto the cathode with a spherical lens and a pair of Littrow prisms which compensate for the anamorphic magnification introduced by the 72^o incidence on the cathode. The time slew across the cathode caused by this oblique incidence is corrected by using a diffraction gradient. The relay imaging technique used throughout the optical transport improves the beam pointing stability. Since the laser beam overfills the limiting aperture, the transverse profile of the beam a truncated gaussian. The spot size of the laser beam on the cathode is 2 mm diameter edge to edge.

2 Injector Design

The NGP consists of the symmetrized BNL/SLAC/UCLA 1.6 cell S-band photocathode RF gun mated to a single emittance compensation solenoidal magnet.

The 1.6 cell RF gun differs from the original BNL 1.5 cell RF gun[2] in that the half cell has been lengthened to decrease the RF field levels on the cell to cell coupling iris and also to provide more RF focusing in the iris region. The 1.6 cell RF gun is not a side coupled 0-mode suppressed RF gun, as in the previous BNL type RF guns. High power RF is coupled only into the full cell. The enlarged beam iris diameter increases the cell to cell coupling, which provides a mode separation between the π and 0-modes of 3.225 MHz for a balanced field configuration. The half cell is fully symmetrized with two 72^o oblique incidence laser ports. The cathode plate is removable using a single helico flex seal for both the vacuum and RF seals. This removable cathode plate eliminates the multipacktering problem common to choke joint cathodes. The removable cathode allows for easy replacement of different cathode materials such as Cu and Mg. The Cu cathode results are presented in this paper. The full cell has two symmetrized plunger type tuners with a tuning range for both tuners of ± 2 MHz. The RF coupling slot is symmetrized by an identical coupling slot that provides additional vacuum pumping.[3] The 1.6 cell gun uses resistive heating to maintain the resonant frequency.

The single emittance compensation solenoidal magnet, that was specifically designed to be used with the 1.6 cell gun, utilizing POISSON[4] field maps into PARMELA[5] to study the beam dynamics consideration of different magnet designs. In previous emittance compensation system designs, a bucking coil is positioned upstream of the cathode plane to null the magnetic field at the cathode. This is unnecessary in the present design since the

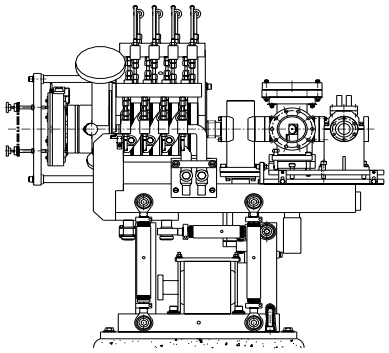

Figure 1: Next Generation Photoinjector

single solenoid magnet produces less than 9 gauss at the cathode when the peak solenoidal field is 3 Kgauss.

After rf conditioning the 1.6 cell RF gun operates at 5x10^{-9} torr with a field gradient of 125 $\frac{MV}{m}$ and in the quiescent state the vacuum is 1x10^{-9} torr.

3 Gun Energy / Dark Current

The BNL/SLAC/UCLA 1.6 cell S-band photocathode RF gun is designed to attain a field level at the cathode and at the middle of the full cell of up to 150 $\frac{MV}{m}$, and to operate with RF pulse widths up to 3.5 μs. Calibration of the field levels in the gun were verified by measurements of the beam energy using a cos(θ) deflection magnet located inside the bore of the emittance compensation solenoidal magnet. The results of these energy measurements are shown in figure 2 where Φ is the laser injection phase. $\Phi = 0$ and $\Phi = 90$ is the zero crossing and crest of the rf respectively.

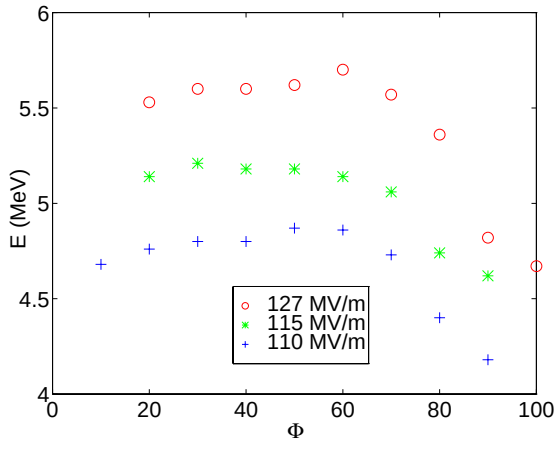

Figure 2: Energy versus Field Level

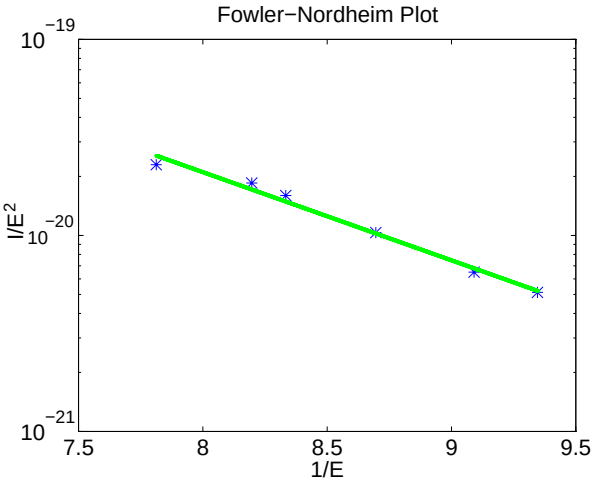

Figure 3: Fowler-Nordheim Plot

Standard machining and Cu wool polishing techniques were used to manufacture both the full and half cells.

The cathode plate was prepared using the procedures detailed in reference.[6] These techniques, when combined together, produce a field enhancement factor $\beta = 58$ as can be seen in the Fowler-Nordheim Plot of figure 3.

4 Multi-Pole Fields

Multi-pole field effects were studied by decreasing the laser spot size to 400 μm and setting the laser injection phase to the Schottky peak. This injection phase causes an effective electron bunch lengthening and a noticeable energy spread tail was observed. By adjusting the laser spot position we were able to eliminate this energy spread tail. This alignment minimizes the integrated higher order mode contribution to the beam distortion. Analysis indicates that the symmetrized BNL/SLAC/UCLA 1.6 cell photocathode RF guns electrical and geometric center are within 170 μm of each other, which is within the laser spot alignment error. Compared to similar experimental results of the 1.5 cell BNL gun whose electrical and geometric centers differ by 1.0 mm,[7] the 1.6 cell gun has fulfilled the symmetrization criteria. Future work with custom laser masks to study the field patterns at larger diameters are planned for the future.[8]

5 Quantum Efficiency versus Polarization

The laser time slew correction has the draw back of decreasing the available laser energy at the cathode by 50%. The available charge was measured as a function of polarization. In figure 4 it can be seen that the charge is maximized at a polarizer angle of 56^o which correspondence to P polarized light on the cathode.

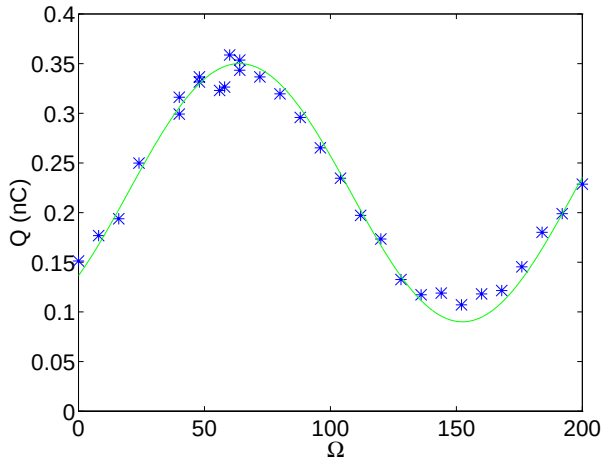

Figure 4: Electron Bunch Charge versus Polarizer Angle

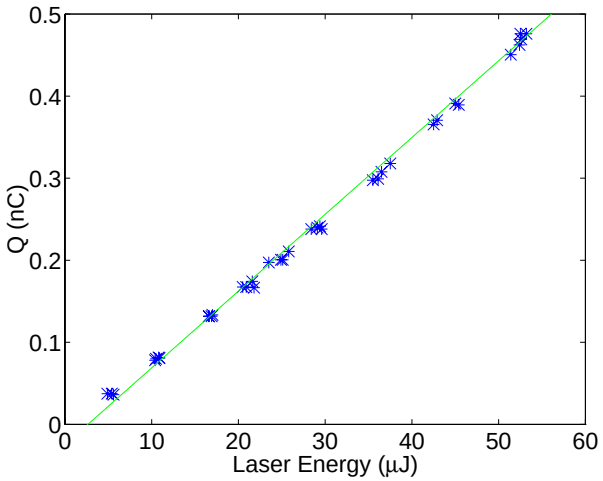

Figure 5: Electron Bunch Charge versus Laser Power

The measured value of the Cu cathode's quantum efficiency is QE = 4.4x10^{-5} which is calculated from figure 5. These studies were conducted at a laser injection phase of 90^o which utilized the Schottky effect to increase the available charge.

$\epsilon_{n,rms}$ Quad Scan	2.29 π mm-mrad
$\epsilon_{n,rms}$ Two Screen	2.42 π mm-mrad

Table 1: Quad Scan and Two Screen Method Results

6 Transverse Phase Space

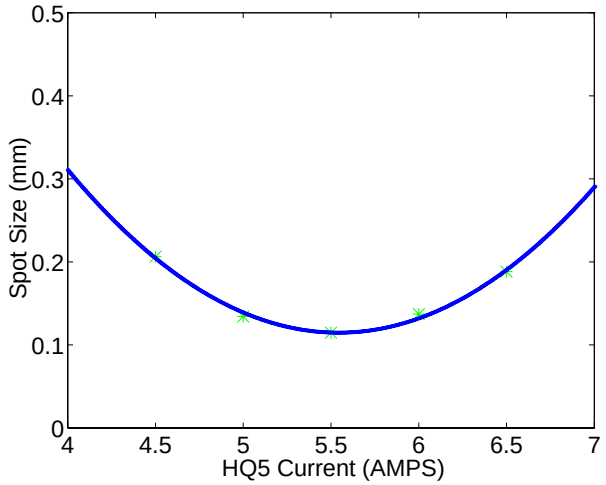

Figure 6: Quadrupole Scan RMS Emittance Results

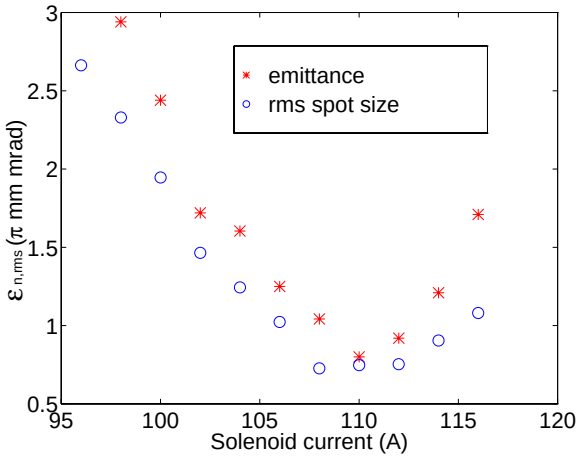

Figure 7: Emittance and RMS Beam Size versus Solenoidal Field

The normalized rms emittance, $\epsilon_{n,rms}$, measurements were taken using a variation of the three screen method. Two screens were utilized while insuring that a beam waist was located at the down stream profile screen. The two screen method is compared to the standard quadrupole scan technique in figure 6 and the results from these two methods are compared in table 1

PARMELA was used to simulate the emittance compensation process and the subsequent acceleration to 40 MeV.[9] A correlation of the minimum spot size with an emittance minimum was noted during these simulations. This was experimentally verified during the commissioning of the 1.6 cell RF gun, using the beam profile monitor located at the output of the second linac section, as can be seen in figure 7. These results are consistent with similar results of the BNL 1.5 cell RF gun.[7]

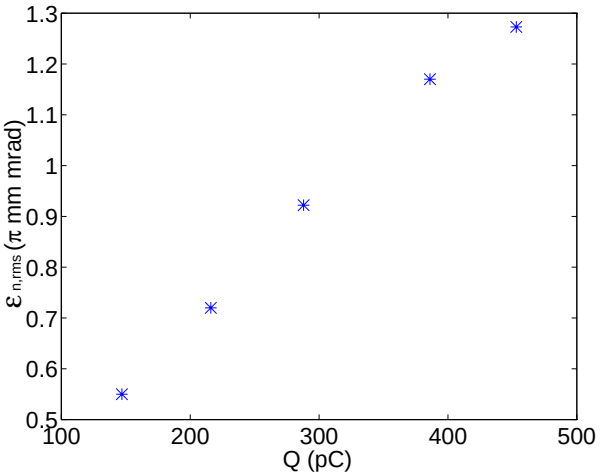

Figure 8: Emittance versus Electron Bunch Charge

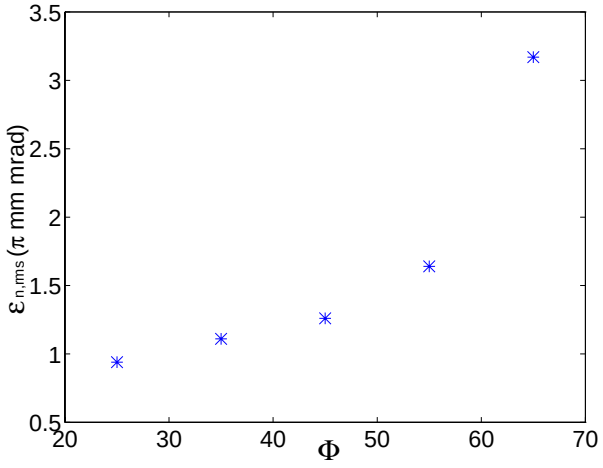

Figure 9: Emittance versus Electron Bunch Charge

There are four emittance terms that contribute to the total $\epsilon_{n,rms}$ these are the space charge, rf, thermal and magnetic terms. The last term is due to the small but finite magnetic field at the cathode.

Studying the dependence of transverse emittance on the bunch charge in figure 8, we have noted that at Q = 0 charge there is a residual emittance term of 0.2 π mm-mrad. This term is due to ϵ_{rf}, $\epsilon_{thermal}$, ϵ_{mag} and measurement errors. If we neglect the magnetic term, which is reasonable due to the initial cathode spot size and the small magnetic field at the cathode we can estimate the thermal and RF emittance terms to be less than 0.2 π mm-mrad. Since the measured $\epsilon_{n,rms}$ is a factor of three less than the ϵ_{sc} that Kim's theory[10] predicated, we are confident that we have produced an emittance compensated beam.

Due to laser power limitation, RF gun bunch compression and the Schottky effect it is not possible to keep the peak current constant for different laser injection phases. Therefore in figure 9 the plot is not for a constant current but for a decreasing charge from a maximum of 400 pC to a minimum of 178 pC. The functional dependence of this plot has been verified by comparison with Kim's theory.

7 Longitudinal Phase Space

When measuring the bunch length and energy spread of the electron bunch the RF system is adjusted such that the bunch initially has a minimum energy spread. This is accomplished by adjusting the overall linac phase with respect to the laser injection phase by means of the low level RF system. The $\delta\phi$ between the two linac section is adjusted by means of a high power RF phase shifter, such that the energy spread of the beam is minimized. The beams energy is set to 40 MeV by adjusting the low level RF drive to the linac klystrons.

The energy spread is estimated by measuring the beam size on a phosphor screen in the dispersion region. The dispersion in this region is 5.4 $\frac{mm}{\%}$. Figure 10 is a plot of the energy spread of the electron bunch as a function of the phase difference between the linacs.

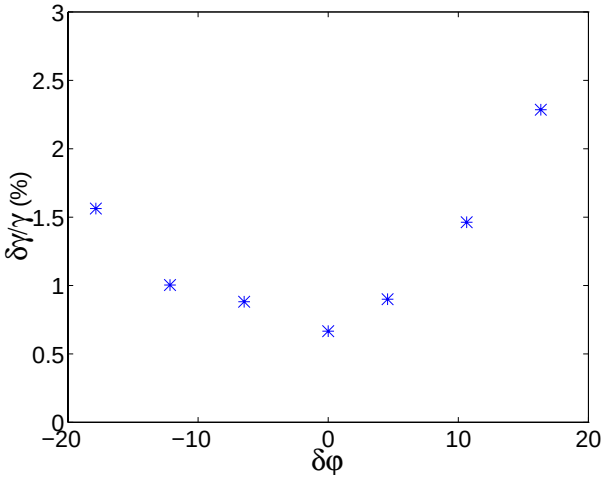

Figure 10: Energy Spread versus Linac Phase

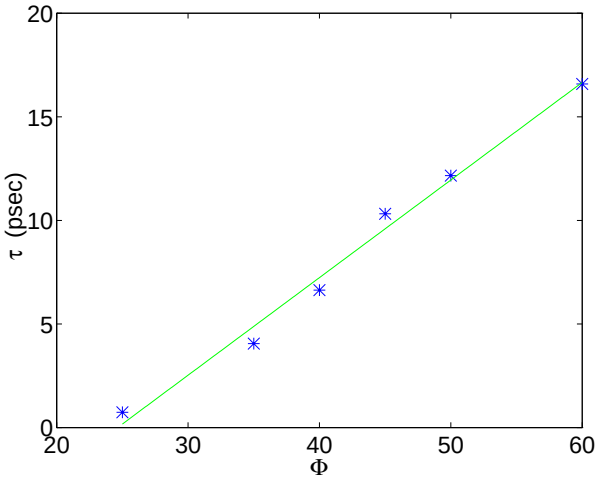

Figure 11: Bunch Length versus Laser Injection Phase

Electron bunch length was measured by dephasing the second linac section such that a linear energy chirp is produced along the bunch. This allows the bunch length to be correlated to the energy spread. Using the technique discussed previously to measure the energy spread, the bunch length is measured as a function of laser injection phase. Figure 11 is experimental verification of bunch compression in the 1.6 cell RF gun. Bunch compression in RF guns have been experimentally demonstrated previously.[11]

8 Conclusions

We have experimentally studied the six dimensional phase space of the electron beam that is produced by the BNL/SLAC/UCLA 1.6 cell S-band photocathode RF gun. We have experimentally verified longitudinal bunch compression, electron bunch energy and transverse emittance as a function of injection phase, solenoidal field and charge for peak fields in the RF gun of $127\frac{MV}{m}$. The optimized rms normalized emittance for a charge of 300 pC is 0.7 π mm-mrad.

Future work includes studies of the multi-pole fields that this gun is designed to suppress, cathode magnetic field effects, along with slice emittance and inverse RADON transforms that will elucidate the electron beams transverse phase space. Emittance measurements for a bunch charge of 1 nC are also planned.

9 Acknowledgments

The authors would like to thank the technical staff at UCLA, the Stanford Linear Accelerator Center and at Brookhaven Accelerator Test Facility for all their dedicated work on this project. We would also like to thank Mr. James N. Weaver from SSRL for all the technical discussions and help that he has provided.

10 REFERENCES

[1] B. E. Carlsten, *NIM*, **A285**, 313 (1989)

[2] K. Batchelor *et al.*, Proc. of 1990 EPAC p. 541

[3] D. T. Palmer *et al.*, Proc. 1995 Part. Accel. Conf. (1995) p. 982

[4] K. Halbach and R. F. Holsinger, *Particle Accelerators* **7**, 213 (1976)

[5] L. M. Young, private communications

[6] T. Srinivasan-Rao *et al.*, BNL-62626

[7] X. J. Wang *et al.*, Proc. 1995 Part. Accel. Conf. (1995) p. 890

[8] Z. Li, private communications

[9] D. T. Palmer *et al.*, Proc. 1995 Part. Accel. Conf. (1995) p. 2432

[10] K. J. Kim, *NIM*, **A275**, 201 (1989)

[11] X. J. Wang *et al.*, Phys. Rev. E, Oct 1989